Helix Packing and Orientation in the Transmembrane Dimer of gp55-P of the Spleen Focus Forming Virus

Wei Liu,* Evan Crocker,† Stefan N. Constantinescu,‡ and Steven O. Smith*
*Department of Biochemistry and Cell Biology, Center for Structural Biology and †Department of Physics and Astronomy, Stony Brook University, Stony Brook, New York 11794; and ‡Ludwig Institute for Cancer Research, Belgium Christian de Duve Institute of Cellular Pathology, MEXP Unit, Université de Louvain, Brussels 1200, Belgium

ABSTRACT gp55-P is a dimeric membrane protein with a single transmembrane helix that is coded by the *env* gene of the polycythemic strain of the spleen focus forming virus. gp55-P activates the erythropoietin (Epo) receptor through specific transmembrane helix interactions, leading to Epo-independent growth of erythroid progenitors and eventually promoting erythroleukemia. We describe the use of magic angle spinning deuterium NMR to establish the structure of the transmembrane dimer of gp55-P in model membranes. Comparison of the deuterium lineshapes of leucines in the center ($Leu^{396–399}$) and at the ends (Leu^{385}, Leu^{407}) of the transmembrane sequence shows that gp55-P has a right-handed crossing angle with Leu^{399} packed in the dimer interface. We discuss the implications of the structure of the gp55-P transmembrane dimer for activation of the Epo receptor.

INTRODUCTION

Activation of membrane receptors is a common strategy used by retroviruses to induce cell proliferation. The polycythemic strain of the spleen focus forming virus (SFFV) encodes a dimeric transmembrane (TM) viral glycoprotein, gp55-P (1–3), which is responsible for the initial proliferative stage of erythroleukemia (1,4–8). gp55-P is able to induce cell proliferation by constitutively activating the erythropoietin (Epo) receptor (1,9–11), a member of the cytokine receptor superfamily that regulates erythrocyte maturation (12).

Both gp55-P and the Epo receptor are integral membrane proteins that span membrane bilayers with a single TM helix. Both proteins are dimeric, and they interact with one another to form a stable complex in the membranes of erythroid progenitors infected by SFFV (9,13–16). Genetic studies have shown that the TM domain and the small C-terminal juxtamembrane region of gp55-P are required for complex formation with the Epo receptor and signaling (1,12,17,18). Moreover, these regions of gp55-P are required for leukemogenicity (6,19). The observation that the interaction between gp55-P and the Epo receptor involves their TM sequences means that gp55-P interacts with the Epo receptor in a distinctly different fashion from the Epo ligand, which binds to the extracellular domain of the receptor.

Evidence for the role of the TM domain in the activation of the Epo receptor comes from comparing variant strains of the SFFV and from mutational studies on gp55-P. Both the polycythemic (P) and anemic (A) strains of the SFFV induce erythroleukemia in adult mice. However, only gp55-P causes Epo-independent proliferation of hematopoietic cell lines (8). Moreover, although both gp55-A and gp55-P are able to specifically bind to the TM domain of the Epo receptor, only gp55-P promotes proliferation and differentiation of early erythroid progenitors, the burst forming unit-erythroids (20). These differences between gp55-A and gp55-P can be traced to their TM sequences, which only differ at six positions (6,8).

How do the six TM sequence differences between gp55-P and gp55-A lead to functional differences between these two similar viral proteins? In principle, the sequence differences may cause changes in how the TM helices interact with one another within a gp55 dimer or in how the gp55 dimer interacts with the Epo receptor dimer. Both gp55-A and gp55-P are homodimers when expressed on the cell surface (21) as a result of disulfide bond formation between cysteines in their extracellular domains (2). However, only the TM domain of gp55-P forms homodimers when assayed by the ToxR chloramphenicol acetyltransferase reporter system (21). This suggests that the ability of gp55-P to activate the Epo receptor is related, at least in part, to the ability of the TM sequence of gp55-P to mediate tight helix-helix interactions.

The human Epo receptor is not activated by gp55-P. However, mutation of a single amino acid (Leu^{238}) in the TM domain of the human receptor to serine, its counterpart in the mouse, allows it to be activated by gp55-P (22). The converse mutation ($Ser^{238}Leu$) in the mouse receptor eliminates its ability to be activated, indicating that Ser^{238} enables gp55-P activation of either the human or mouse receptor. Based on computational searches, we proposed that Met^{390} of gp55-P interacts specifically with Ser^{238} to activate the receptor (22). Mutation of Met^{390} to isoleucine (the amino acid at position 390 in gp55-A) eliminates the ability of gp55-P to activate human ($Leu^{238}Ser$) and mouse Epo receptors (22). In

Submitted December 13, 2004, and accepted for publication April 25, 2005.
Address reprint requests to Steven O. Smith, Dept. of Biochemistry and Cell Biology Z = 5215, Stony Brook University, Stony Brook, NY 11794-5215; Tel.: 631-632-1210; Fax: 631-632-8575; E-mail: steven.o.smith@sunysb.edu.

0006-3495/05/08/1194/09 $2.00
doi: 10.1529/biophysj.104.057844

addition, the $M^{390}L$ mutation was reported to induce anemia, rather than polycythemia (23). These observations suggest that the sequence differences between gp55-P and gp55-A also result in changes in specific TM contacts between gp55-P/A and the Epo receptor.

Here, we use deuterium NMR spectroscopy in combination with magic angle spinning (MAS) to determine the structure of the gp55-P TM dimer. The dimer structure provides a framework for establishing the mechanism for how the TM region of gp55-P activates the Epo receptor, as well as for understanding how sequence differences in mutant viral proteins confer different phenotypes. Deuterium NMR spectroscopy takes advantage of the sensitivity of deuterium lineshapes to molecular motion (24–26). We have previously shown that the motion of amino acids located in TM helix interfaces is restricted relative to amino acids oriented toward the lipid membrane (27). As a result, by characterizing side-chain motion as a function of the TM sequence, one can map out the interface of interacting TM helices. Typically, deuterium NMR lineshape analyses are carried out on static samples and have been used extensively to study lipid motion (28). Studies of membrane proteins have been limited by low sensitivity. To overcome this problem, we take advantage of the increased sensitivity afforded by MAS to observe changes in the quadrupolar lineshape. We propose that deuterium MAS of consecutive leucine side chains in a TM sequence provides a simple approach for studying helix-helix interactions in membrane proteins. Together with results from polarized infrared (IR) spectroscopy and computational searches, the deuterium MAS spectra of specifically deuterated leucines in the TM sequence of gp55-P are used to establish its TM dimer structure.

EXPERIMENTAL PROCEDURES

Materials

Deuterated (5,5,5-D_3) leucine and deuterium-free water were purchased from Cambridge Isotope Laboratories (Andover, MA). Other amino acids and octyl-β-glucoside were obtained from Sigma Chemical (St. Louis, MO). DMPC was obtained from Avanti Polar Lipids (Alabaster, AL) as a lyophilized powder and used without further purification.

Peptide synthesis and purification

Peptides (33 residues in length) corresponding to the TM domain of gp55-P were synthesized using solid-phase methods at the W. M. Keck Peptide Synthesis Facility at Yale University. The sequence is largely hydrophobic with Arg and Trp/His defining the N-terminal and C-terminal boundaries of the TM domain, respectively.

The crude peptide (5–15 mg) was purified by reverse-phase high-performance liquid chromatography on a C4 column using gradient elution. The gradient starts with a largely aqueous solution of 70% distilled water, 12% acetonitrile, and 18% 2-propanol and is changed to a more hydrophobic composition of 40% acetonitrile and 60% 2-propanol that elutes the peptides. The elution was monitored by the optical absorbance at 260 nm. The solutions corresponding to the peaks were collected into several fractions that were then lyophilized and checked by mass spectrometry for purity.

Purified gp55-P peptides were reconstituted by detergent dialysis by first dissolving DMPC, lyophilized peptide, and detergent (octyl-β-glucoside) in trifluoroethanol. This mixture was incubated at 37°C for over 2 h, and the trifluoroethanol was removed by evaporation using a stream of argon gas and then placing the sample under vacuum. The dry mixture was rehydrated with phosphate buffer (10 mM phosphate and 50 mM NaCl, pH 7.4), such that the final concentration of octyl-β-glucoside was 5% (w/v). The rehydrated sample was then stirred slowly for at least 6 h, and the octyl-β-glucoside was removed by dialysis using Spectra-Por dialysis tubing (3500 MW cut off) for 24 h against phosphate buffer at 37°C. The samples were then pelleted, lyophilized, and rehydrated with deuterium-depleted water (50 $\pm$ 5% weight) and incubated at 37°C for 24 h. The reconstituted membranes were pelleted to form multilamellar dispersions and loaded into NMR rotors.

To characterize the influence of the hydration level on the deuterium spectrum, parallel samples were run of Leu^{396} at 40% and 60% deuterium-depleted water (by weight). The relative intensities of the MAS side bands were not significantly different between these samples (data not shown).

Polarized IR spectroscopy

Polarized attenuated total reflection (ATR) Fourier transform infrared (FTIR) spectra were obtained on a Bruker IFS 66V/S spectrometer. Multilamellar vesicle dispersions at a concentration of 10 mg lipid/mL were layered on a germanium internal-reflection element using a slow flow of air directed at an oblique angle to the ATR plate to form an oriented multilamellar lipid-peptide film. Each sample spectrum represents the average of 1000 scans acquired at a resolution of 4 cm^{-1}.

The dichroic ratio (R^{ATR}) is defined as the ratio between absorption of parallel ($A_{\|}$) and perpendicular ($A_{\perp}$) polarized light (29). The observed dichroic ratio is used to calculate the order parameter S_{meas} using the equation,

$$S_{meas} = \frac{E_x^2 - R^{ATR}E_y^2 + E_z^2}{E_x^2 - R^{ATR}E_y^2 - 2E_z^2} = \left[\frac{3\cos^2\theta - 1}{2}\right]\left[\frac{3\cos^2\alpha - 1}{2}\right]S_{mem}. \quad (1)$$

Order parameters (S_{meas}) of 1.0 and -0.5 correspond to helical orientations parallel and perpendicular to the membrane normal, respectively. The order parameter depends on the electric field amplitudes, $E_x = 1.399$, $E_y = 1.514$, and $E_z = 1.621$, in the thick film limit which is applicable for our experiments. θ is the angle between the helix director and the normal of the internal-reflection element, and α is the angle between the helix director and the transition-dipole moment of the amide I vibrational mode.

To calculate the angle θ between the helix director and the normal of the ATR plate, one must know the value of the transition moment angle α. There has been a wide range of values for α reported in the literature over the years (e.g., from 20° (30) to 40° (31)) due to the lack of good model systems for polarized IR studies where the orientation and disorder of the amide bonds were known independently from the IR measurements. Recently, Marsh and co-workers have converged on a value of α in two very different systems: 38° for a block co-polymer poly(γ-methyl-L-glutamate)$_x$-co-(γ-*n*-octadecyl-L-glutamate)$_y$ (32) and 39.5° for the membrane protein bacteriorhodopsin (33). These results indicate that the transition moment angle for the amide I vibration is independent of the specific system used. Importantly, Marsh and Pali (33) show that there are only limited structural deviations between the TM helices of bacteriorhodopsin and a standard α-helix. Consequently, the value of 39.5° obtained for bacteriorhodopsin is applicable to standard helices.

We typically obtain polarized IR spectra of bacteriorhodopsin before measurements on reconstituted TM peptides. This approach provides an independent check of our experimental setup and validates the use of 39.5° for the transition moment angle α. Bacteriorhodopsin is an integral membrane protein that forms two-dimensional crystalline arrays that orient well on germanium ATR surfaces. The disorder in orientation typically corresponds

to an S_{mem} of 0.8–0.9 based on measurements of mosaic spread (30). Since we cannot independently measure the disorder in the orientation of our reconstituted TM peptides, we use a value of S_{mem} equal to 0.85 as the upper limit in our calculations. We assume that the disorder in the gp55-P sample is equal to the disorder in bacteriorhodopsin. If the disorder is greater in our reconstituted sample, then the measured dichroic ratio will be less than the true dichroic ratio, and the true crossing angle will be smaller for the gp55-P helices.

One way to indirectly assess the quality of our reconstitutions is to measure the dichroic ratios of the lipids. Dichroic ratios of the asymmetric and symmetric lipid CH_2 stretching modes at 2924 cm^{-1} and 2852 cm^{-1} were 1.15 and 1.10, respectively, which correspond to order parameters of 0.65 and 0.67, and are consistent with well-oriented lipids (34).

NMR spectroscopy

Deuterium NMR spectra were obtained at a ^2H frequency of 55.26 MHz using MAS. MAS spectra yield much higher sensitivity compared to conventional static spectra in membrane-reconstituted samples where the concentration of deuterated peptide is low. A MAS frequency of 3 kHz was used to have a sufficient number of spinning side bands to define the static lineshape. Single pulse excitation was employed using a 3.7-μs 90° pulse, followed by a 4.5-μs delay before data acquisition. The repetition delay was 250 ms. A total of 600,000–800,000 transients were averaged for each spectrum and processed using a 200-Hz exponential line broadening function. Spectra were obtained at 25°C.

MAS deuterium spectra were simulated using the program SIMPSON version 1.1.0 (35) with a spin rate of 3.0 kHz. The asymmetry parameter, η, was set to 1.0. Only the quadrupole coupling constant was varied to quantify the breadth of the lineshape.

Computational searches

The computational search strategy using the program CHI has been described previously (36). Low-energy conformations of helix dimers were searched by rotating each helix through rotation angles ϕ_1 and ϕ_2 from 0° to 360° with sampling step sizes of 25°–45° and with interhelical separations of 9.5 Å, 10.0 Å, and 10.5 Å. The ϕ_1 and ϕ_2 angles are equivalent to the α and β angles originally described by Adams et al. (36). Molecular dynamics simulations were run with simulated annealing at each rotational orientation of the dimer using the program X-PLOR along with the united atom topology and parameters sets, TOPH19 and PARAM19, respectively. Calculations were carried out for helices with both left-handed (LH) and right-handed (RH) geometries with initial crossing angles of 25°. Four different runs were carried out for each starting geometry using torsional angle dynamics. The rotation and crossing angles were allowed to vary during the simulations. To maintain an α-helical conformation, distance restraints were applied between O_i and N_{i+4} atoms along the backbone.

RESULTS AND DISCUSSION

Peptides corresponding to the TM domains of membrane proteins are able to independently fold and associate in membrane bilayers (37). To determine the structure of the TM dimer of gp55-P, we first establish that gp55-P TM peptides adopt an α-helical TM conformation in bilayers using polarized IR spectroscopy. Second, deuterium NMR spectroscopy of gp55-P containing specifically ^2H-labeled leucine is used to establish the rotational orientation and crossing angle of the TM helices. Third, computational searches are undertaken to generate possible low-energy dimer structures that are consistent with the IR and NMR data.

TM α-helical structure of gp55-P

Fig. 1 presents polarized IR spectra of the TM domain of gp55-P reconstituted into model dimyristoylphosphocholine (DMPC) bilayers. The amide I vibration is observed at 1657 cm^{-1}, a frequency characteristic of α-helical secondary structure. Fourier deconvolution of the amide I band reveals no significant nonhelical structure. The dichroic ratio of the amide I band is sensitive to the orientation of the gp55-P helix relative to the plane of membrane. The observed dichroic ratio of 3.0 corresponds to a helix orientation of ~25° relative to the membrane normal (see Methods). These data indicate that peptides corresponding to the gp55-P TM domain are reconstituted into DMPC bilayers in a helical TM conformation.

Deuterium MAS NMR of ^2H-leucine as a probe of TM helix interactions

There are several advantages of deuterium MAS spectroscopy as a structural method for mapping out the helix interfaces of oligomeric membrane peptides and proteins. The first advantage is that the NMR experiment used here is simple. Only one-dimensional deuterium NMR spectra need to be acquired. The pulse sequence consists of a single pulse on the deuterium channel without proton decoupling. Second, MAS greatly increases the sensitivity of the experiment, which allows one to study peptides embedded into membrane bilayers at low concentration. Moreover, the MAS frequencies are slow and are readily attainable with standard MAS probes. The third advantage is that the data can be acquired over a broad temperature range, above and below the lipid phase transition temperatures. In contrast, distance measurements using rotational resonance or rotational echo double resonance techniques are best done at low temperature where the full dipolar couplings can be measured.

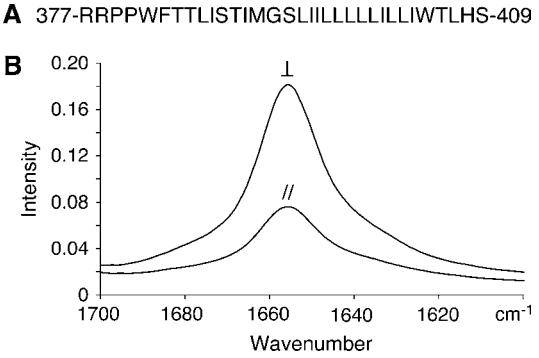

FIGURE 1 (*A*) Sequence of the TM domain of gp55-P. (*B*) Polarized IR spectra of gp55-P TM peptides reconstituted into DMPC bilayers exhibit an amide I vibration at 1657 cm^{-1} and a dichroic ratio of 3.0. These data indicate that the gp55-P TM domain has α-helical secondary structure with the helix axis oriented roughly perpendicular to the membrane surface.

Previous deuterium NMR studies of side-chain motion in TM helices have focused on leucine (25), valine (27), and alanine (26). Leucine containing a single deuterated methyl group (5,5,5-^{2}H-Leu) has several advantages over other deuterated amino acids for probing molecular motion. First, leucine is the most abundant amino acid in TM helices (38). There are often strings of consecutive leucines in membrane spanning sequences, allowing side-chain motion on different faces of a helix to be compared in a sequential manner. Second, leucine has a long flexible side chain (Cα-Cβ-Cγ-CD_3). The high degree of flexibility of the side chain results in a large difference in the deuterium spectrum of leucine restricted in a helix interface when compared to leucine oriented toward a lipid interface. In contrast, the side chain of alanine is much less flexible. The alanine methyl group has a defined orientation relative to the helix backbone and is only averaged by rotation about the Cα-Cβ bond. For valine, steric interactions between the side chain methyl groups and the backbone restrict motion about the Cα-Cβ bond. Only subtle differences are observed in the lineshapes of valines located in interfacial and noninterfacial positions (27).

The approach taken here is to compare spectra of deuterated leucines at different positions in the gp55-P TM helix in parallel samples. For instance, four consecutive leucines (e.g., Leu^{396}-Leu^{397}-Leu^{398}-Leu^{399}) in the TM sequence constitute one full turn of the gp55-P α-helix. At least one of the leucine side chains will be facing the helix dimer interface and exhibit a broader deuterium spectrum due to restricted motion.

The intensities of the side bands in the MAS deuterium spectra trace out the broad deuterium lineshapes. The high flexibility, which makes deuterated leucine a sensitive probe of molecular motion, limits analyses of the deuterium lineshape by detailed spectral simulation. To quantify the observed differences in the width of these lineshapes, we simulate the MAS deuterium spectra using the quadrupole coupling constant as the only free parameter. The simulations assume that the lineshapes have an asymmetry parameter (η) of 1 due to high motional averaging (39). Importantly, the simulations are simple to run using a program that is readily available (http://nmr.imsb.au.dk/bionmr/software/simpson.php).

Leu^{399} is in the gp55-P TM dimer interface

The strategy to determine the interface of the gp55-P dimer is to target a consecutive stretch of leucines in the middle of the TM domain: Leu^{396}-Leu^{397}-Leu^{398}-Leu^{399}. The string of consecutive amino acids facilitates a direct comparison. The left column of Fig. 2 shows the deuterium spectra of the gp55-P TM peptides labeled at Leu^{396} through Leu^{399}. The large central resonance in the spectrum is due to residual ^{1}H^{2}HO. The sharp MAS side bands are spaced at the spinning frequency (3 kHz) and trace out the envelope of the deuterium lineshape. Comparison of the deuterium lineshapes (i.e., the broad envelopes traced out by the intensities of the MAS side bands) in Fig. 2 shows that the lineshape of Leu^{399} is considerably broader than Leu^{396}, Leu^{397}, or Leu^{398}. The broader lineshape of Leu^{399} is indicative of restricted motion compared to the other three leucines, which in turn implies that Leu^{399} is located in the dimer interface. Leu^{396} and Leu^{398} are more restricted than Leu^{397}, consistent with their packing against Leu^{399} (see structural model below).

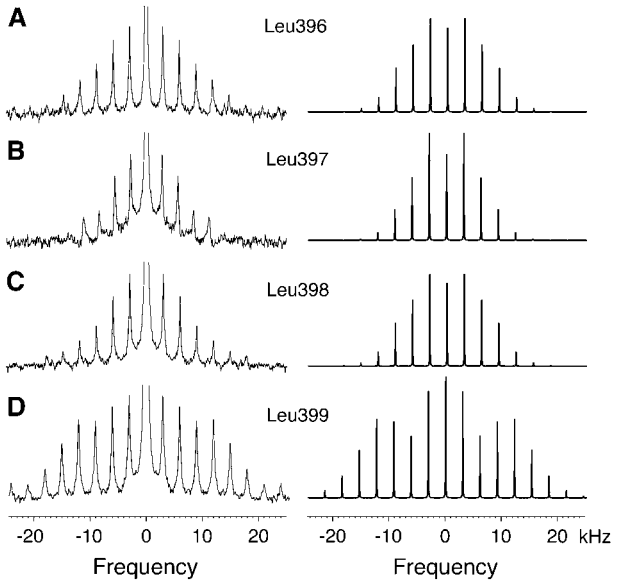

FIGURE 2 Deuterium MAS NMR spectra and simulations of gp55-P deuterium labeled at Leu^{396}-Leu^{399} (*A–D*). The MAS spectra were obtained at 3 kHz and a temperature of 25°C. Each spectrum represents the average of 600,000–800,000 transients. Exponential line broadening of 200 Hz was applied. The simulations to the right were carried out using the program SIMPSON version 1.1.0 (35). The MAS rate was set to 3 kHz, and the asymmetry parameter was set to 1.0. The best fits to the observed side band intensities were obtained using quadrupole coupling constants of 16 kHz (*A*), 14 kHz (*B*), 16 kHz (*C*), and 25 kHz (*D*).

The width of the deuterium lineshape is modulated by rotations about the Cα-Cβ, Cβ-Cγ, and Cγ-CD_3 bonds of leucine. The right column of Fig. 2 presents simulations of the experimental ^{2}H spectra that quantify the differences in lineshape using an asymmetry parameter of 1.0 and varying the quadrupolar coupling constant to obtain the best fit to the observed side band intensities. Based on the simulations, Leu^{397} has the narrowest lineshape with a quadrupolar coupling constant of 14 kHz, whereas Leu^{399} has the broadest lineshape with a quadrupolar coupling constant of 25 kHz.

The gp55-P TM dimer has an RH crossing angle

Comparison of the deuterium spectra in Fig. 2 indicates that Leu^{399} is in the dimer interface of gp55-P. With a single point of contact in the center of the TM sequence, one can

establish the full dimer interface if one knows whether the helices cross with an LH or RH crossing angle. Both types of configurations are common in membrane proteins (40). The crossing angle of the two helices in the gp55-P dimer can be determined based on deuterium spectra of leucines that are positioned at the ends of the TM helices. If Leu^{399} is in the interface and roughly at the crossing point of the two helices in the center of the TM sequence, then the position of Leu^{385} and Leu^{407} with respect to the interface will depend on the crossing angle (Fig. 3). If Leu^{399} is in an interfacial ''a'' or ''d'' position of an LH coiled coil, then Leu^{385} would lie in an ''a'' or ''d'' position. In contrast, Leu^{407} would lie in a ''b'' or ''e'' position outside of the dimer interface. In a similar fashion, in an RH geometry with Leu^{399} in the interface, Leu^{385} would be oriented toward the lipid and Leu^{407} would lie in the dimer interface.

The left column of Fig. 4 compares the deuterium NMR spectra of Leu^{385} and Leu^{407}. The spectrum of Leu^{385} is similar to that of Leu^{396}, which is in a lipid-facing position, whereas the spectrum of Leu^{407} is similar to that of Leu^{399} in the dimer interface. The broader lineshape observed for Leu^{407} is best fit with a quadrupole coupling constant of 27 kHz. The lineshape is consistent with an RH geometry and argues that the gp55-P remains helical through Leu^{407}, which is located in the short juxtamembrane sequence of the protein.

Finally, the helix tilt determined from polarized IR experiments supports the conclusion from the deuterium NMR measurements that the gp55-P helices have an RH crossing angle. Based on packing considerations alone, the crossing angles for RH and LH helices predicted by Chothia (41) are $-52°$ and $+23°$, respectively. The tilt angle of 25° relative to the bilayer normal, inferred from the amide I dichroic ratio, corresponds to a crossing angle of $\sim 50°$ consistent with an RH crossing geometry.

An important point to emphasize here is that the sign of the crossing angle (i.e., RH versus LH) is determined from the NMR data presented in Fig. 4. Comparison of the Leu^{385} and Leu^{407} lineshapes is consistent with an RH crossing angle but is not consistent with an LH crossing angle. An estimate of the magnitude of the crossing angle is derived from the polarized ATR-FTIR data. The calculated crossing angle of $\sim 50°$ is consistent with the NMR determination that the crossing angle is RH. However, as noted in the Methods section the measured dichroic ratio corresponds to the maximum tilt angle of the gp55-P helix. If the reconstitution is not optimal, then the observed dichroic ratio may be lower than the true dichroic ratio. This would yield a smaller crossing angle for the gp55-P helices.

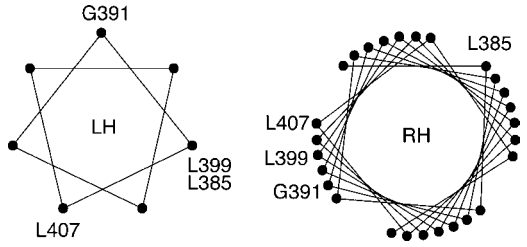

FIGURE 3 Helical wheel plots for helix dimers having LH and RH crossing angles. These diagrams have either 3.5 (LH) or 3.9 (RH) amino acids per turn and provide a truer representation than a canonical helical wheel diagram, of which amino acids line the dimer interface when helices cross with LH or RH crossing angles, respectively. For example, in an LH coiled coil, if Leu^{399} and Leu^{385} are in the dimer interface, then Gly^{391} and Leu^{407} would lie outside of the interface.

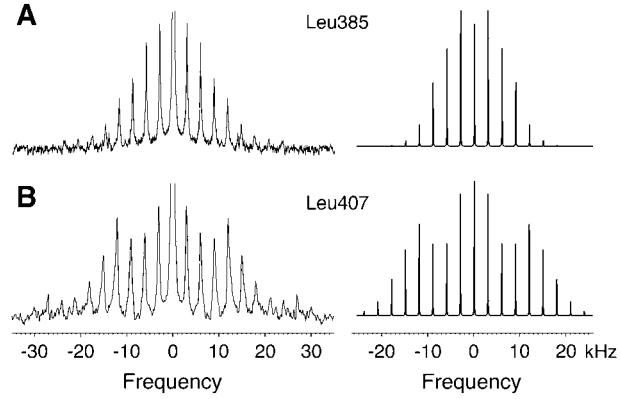

FIGURE 4 Deuterium MAS NMR spectra and simulations of gp55-P deuterium labeled at Leu^{385} and Leu^{407}. The MAS spectra were obtained at 3 kHz and a temperature of 298 K. The spectra of Leu^{385} (*A*) and Leu^{407} (*B*) represent the average of 800,000 and 1,200,000 transients, respectively. An exponential line broadening of 200 Hz was applied. The simulations to the right were carried out using the program SIMPSON version 1.1.0 (35). The MAS rate was set to 3 kHz, the asymmetry parameter was set to 1.0, and the quadrupole coupling constant was changed to 16 kHz and 27 kHz to obtain the best fit to the side band intensities of Leu^{385} and Leu^{407}, respectively.

The deuterium MAS spectra and simulations also serve to emphasize two additional points. First, the simulations assume that the lineshapes have an asymmetry parameter of 1. Both the Leu^{399} and Leu^{407} lineshapes exhibit spectra where the ± 4 side bands have greater intensity than the ± 3 side bands. These features are well reproduced in the simulations and support the assumption of η equal to 1. Second, the Leu^{399} and Leu^{407} lineshapes are remarkably similar. In both cases, the broadening of the lineshape is attributed to restriction of leucine side-chain motion due to packing in the gp55-P dimer interface. This suggests that leucine motion and the associated deuterium MAS analyses are not dependent on the position of the deuterated leucine relatively to the membrane surface.

Structural model of the gp55-P TM dimer

The deuterium NMR data presented in Figs. 2 and 4 provide structural constraints for evaluating models of the gp55-P TM dimer that emerge from computational searches for low-energy helix dimers (36). The NMR constraints were not used to guide or otherwise influence the searches.

In our computational studies, low-energy conformations of gp55-P helix dimers having both RH and LH crossing angles were searched by rotating each helix in the dimer relative to the other (see Methods). Fig. 5 *A* presents the results of a computational search for RH crossing angles. The figure shows only those structures that fall into a ''cluster'', where a cluster is defined as a minimum of five structures with a root mean square deviation of 1 Å or less. These are the final minimized conformations that have migrated from their initial geometries into low-energy wells. Of the initial 512 structures in the computational search, only one symmetric cluster was found with Leu^{399} in the dimer interface (*circled* in Fig. 5). The low-energy structure is robust. Similar structures were found in simulations with helix separations of 9.5 Å, 10.0 Å, and 10.5 Å. The following results are based on a helix-helix separation of 10.0 Å.

The average molecular structure of the low-energy helix dimer from the symmetric cluster is shown in Fig. 6 with

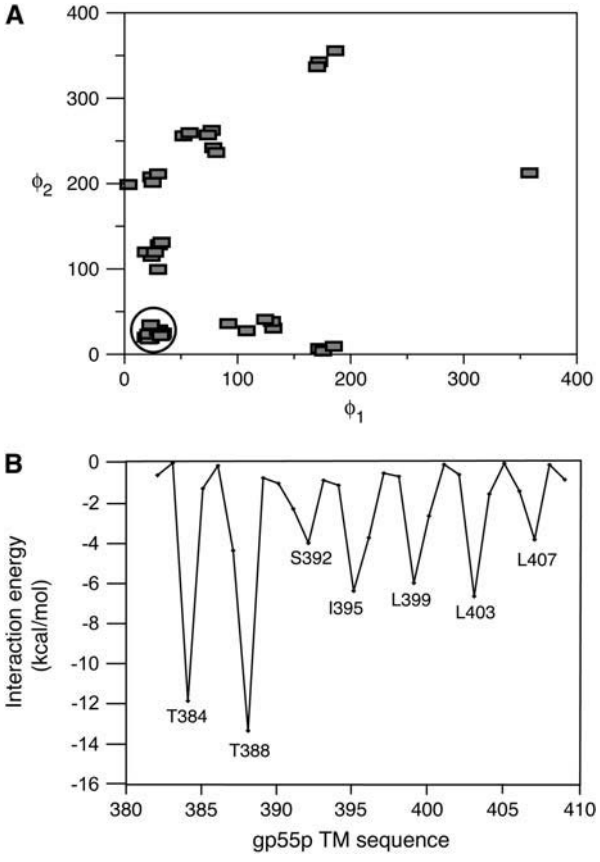

FIGURE 5 Computational searches for low-energy structures of the gp55-P TM dimer. (*A*) Low-energy structures of the gp55-P TM dimer with RH helix crossing angles. The figure plots the final rotational angles of the two TM helices (ϕ_1 and ϕ_2) for those structures that fall into a ''cluster''. Only a single cluster (*circled*) was observed along the diagonal and corresponds to a symmetric dimer structure. No symmetric dimer clusters were observed for comparable searches for gp55-P with LH crossing angles. The interhelical separation for this search was maintained at 10 Å. (*B*) Helix interaction energies for average TM dimer structure from the symmetric cluster.

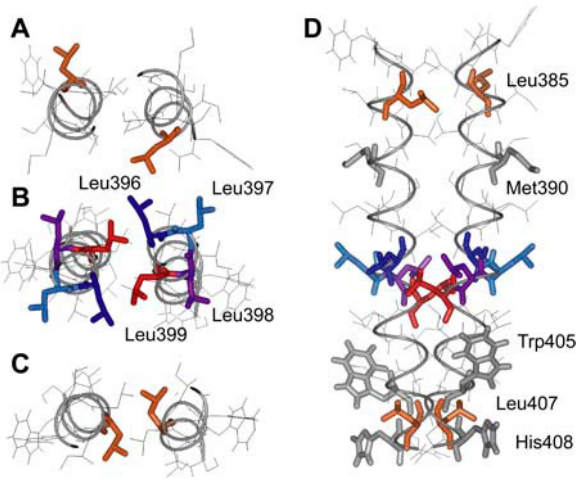

FIGURE 6 Structural model of the gp55-P TM dimer. (*A*) Cross section of the gp55-P dimer showing the noninterfacial position of Leu^{385} (*orange*). (*B*) Cross section of the gp55-P dimer highlighting one helix turn with four consecutive leucines. Leu^{399} (*red*) is in the dimer interface.(*C*) Cross section of the gp55-P dimer showing the interfacial position of Leu^{407} (*orange*). (*D*) gp55-P TM dimer highlighting the leucine residues labeled in this study. Met^{390}, Trp^{405}, and His^{408} are oriented away from the dimer interface. Met^{390} is thought to interact with Ser^{298} of the Epo receptor.

a helix crossing angle of ~35°. The structure provides a framework for interpreting mutational and biochemical data on gp55-P. The working model is that a stable TM dimer structure is required for activation and that amino acids oriented away from the dimer interface interact directly with the TM domain of the Epo receptor.

First, we discuss the amino acids predicted to mediate dimerization of gp55-P. The helix interaction energy for the average molecular structure in the symmetric cluster is shown in Fig. 5 *B*. The low-energy structure is stabilized by hydrogen bonding across the dimer interface of Thr^{384}–Thr^{384} and Thr^{388}–Thr^{388}. In simulations on gp55-P dimers having shorter axial separations (e.g., 9.5 Å), hydrogen bonding of Ser^{392} to the backbone of Gly^{391} was also observed. Decreasing the step-size during some of the conformational searches also yielded clusters that exhibited Gly^{391}-Ser^{392} hydrogen bonding. The observation of Thr, Ser, and Gly in the gp55-P interface is consistent with the role of small and weakly polar amino acids in mediating helix interactions in polytopic membrane proteins (42).

There are two sites in the gp55-P dimer interface, Gly^{391} and Leu^{399}, where mutation blocks the ability of gp55-P to activate the Epo receptor. Gly^{391} is predicted to be in the dimer interface of the RH gp55-P structure (Fig. 3). Mutation of Gly^{391} to leucine blocks the ability of gp55-P to activate the Epo receptor (22). Glycine often serves as a molecular notch for mediating TM helix interactions (43). For instance, in the TM helix dimer of glycophorin A, two glycines are found in the helical interface (29,44), and mutation of either is sufficient to disrupt dimerization (45).

Mutation of Leu^{399} to isoleucine, the corresponding amino acid in gp55-A, also abolishes the ability of gp55-P to activate the Epo receptor (22). The deuterium data in Fig. 2 clearly show that Leu^{399} is well packed in the dimer interface. Whereas the mutation of Leu^{399} to isoleucine is conservative, in glycophorin A, it was found that mutation of Leu^{75}, which is in the dimer interface, to isoleucine was sufficient to disrupt dimerization (45). In the structural model of the gp55-P dimer, replacement of isoleucine for leucine at position 399 results in steric clash between the isoleucine β-methyl groups. The effects of mutations at similar amino acids in the dimer interfaces of gp55-P and glycophorin A suggest that a stable gp55-P dimer structure is required for activation of the Epo receptor.

The TM dimer structure of gp55-P in Fig. 6 shows that several amino acids thought to mediate TM interactions with the Epo receptor are oriented toward the lipid interface. We have previously proposed that Met^{390} is oriented away from the dimer interface and interacts with Ser^{238} in the Epo receptor (22). Mutation of Met^{390} to isoleucine, the corresponding amino acid in gp55-A, abolishes the ability to activate the Epo receptor (22). The gp55-P dimer structure confirms our previous proposal.

The isoleucine in position 404 is not directly in the dimer interface and can tolerate substitution with Leu or Phe (22). However, deletion of Ile^{404} results in loss of gp55-P-induced activation of the Epo receptor (21). The gp55-P dimer structure in Fig. 6 orients Trp^{405}, a large aromatic amino acid, away from the dimer interface. Deletion of Ile^{404} would likely change the orientation of the C-terminal end of the gp55-P helix such that Trp^{405} on opposing helices would rotate toward the dimer interface and clash, possibly disrupting dimerization or the local helical secondary structure. These data suggest that the short C-terminal end of gp55-P also interacts with the Epo receptor. This would not be surprising because the juxtamembrane sequence of the Epo receptor is highly conserved and has been proposed as a switch region for regulating receptor activity (46). The deuterium NMR data, showing that Leu^{407} is well packed in the helical interface of gp55-P, provides compelling evidence that the end of the gp55-P helix is not unraveled and that both Trp^{405} and His^{408} are in a position to interact with the juxtamembrane sequence of the receptor.

The low-energy structure of the gp55-P dimer along with the analysis of the mutations above suggests that the gp55-P dimer structure does not change upon interaction with the Epo receptor. Rather, gp55-P catalyzes the conversion of an inactive Epo receptor TM dimer to an active dimer. Deuterium MAS NMR studies are in progress to directly test this model.

Comparison of gp55-P and gp55-A suggests that novel sequences may in principle be identified that could bind and activate the Epo receptor to different extents. We plan to exploit the productive interaction between the Epo receptor and gp55-P TM domains as a selection system to design and test sequences for their ability to bind the TM domain of the Epo receptor and activate receptor signaling. Such genetic systems have previously been described only for bacteria (47–49) and could lead to new insights into specific TM interactions in mammalian cell membranes.

Finally, the TM sequence of gp55-P is almost identical to that of the fusiogenic envelope proteins of the mink cell focus-inducing viruses and murine leukemia viruses. The major exception is at position 392, where there is a conserved proline in place of Ser in gp55-P and gp55-A (50). Position 392 is relatively tolerant to mutation in gp55-P (S. N. Constantinescu, unpublished results). However, mutation of Pro^{392} to alanine in the fusiogenic envelope proteins blocks viral fusion with the cell membrane but not incorporation of the envelope protein into virions (50). Langosch and coworkers (51) have proposed that structural flexibility introduced by Pro^{392} is required for fusogenicity. The structure of the gp55-P TM dimer provides a basis for understanding how small sequence differences in the TM domain between gp55-P and the viral envelope proteins affect function. The gp55 proteins are not able to mediate membrane fusion but have evolved the capability to activate membrane receptors.

We gratefully acknowledge the W. M. Keck Foundation for support of the NMR facilities in the Center of Structural Biology at Stony Brook. We thank Martine Ziliox for assistance with the NMR experiments and critical reading of the manuscript. We thank Paul Adams and Axel Brünger for the CHI program.

This work was supported by the National Institutes of Health-National Science Foundation instrumentation grants (S10 RR13889 and DBI-9977553), a grant from the National Institutes of Health (GM-46732) to S.O.S., and by grants from the Fonds National de la Recherche Scientifique (FNRS) and the Fédération Belge contre le Cancer and the de Hovre Foundation (SNC) to S.C. S.N.C. is a Research Associate of the FNRS Belgium.

REFERENCES

1. D'Andrea, A. D. 1992. The interaction of the erythropoietin receptor and gp55. *Cancer Surv.* 15:19–36.
2. Gliniak, B. C., S. L. Kozak, R. T. Jones, and D. Kabat. 1991. Disulfide bonding controls the processing of retroviral envelope glycoproteins. *J. Biol. Chem.* 266:22991–22997.
3. Wolff, L., E. Scolnick, and S. Ruscetti. 1983. Envelope gene of the friend spleen focus-forming virus—deletion and insertions in 3′gp70/p15e-encoding region have resulted in unique features in the primary structure of its protein product. *Proc. Natl. Acad. Sci. USA.* 80:4718–4722.
4. Ahlers, N., N. Hunt, U. Just, C. Laker, W. Ostertag, and J. Nowock. 1994. Selectable retrovirus vectors encoding friend-virus gp55 or erythropoietin induce polycythemia with different phenotypic-expression and disease progression. *J. Virol.* 68:7235–7243.
5. Aizawa, S., Y. Suda, Y. Furuta, T. Yagi, N. Takeda, N. Watanabe, M. Nagayoshi, and Y. Ikawa. 1990. Env-derived gp55 gene of friend spleen focus-forming virus specifically induces neoplastic proliferation of erythroid progenitor cells. *EMBO J.* 9:2107–2116.
6. Chung, S. W., L. Wolff, and S. K. Ruscetti. 1989. Transmembrane domain of the envelope gene of a polycythemia-inducing retrovirus

determines erythropoietin-independent growth. *Proc. Natl. Acad. Sci. USA*. 86:7957–7960.

7. Kabat, D. 1989. Molecular-biology of friend viral erythroleukemia. *Curr. Top. Microbiol. Immunol.* 148:1–42.
8. Ruscetti, S., and L. Wolff. 1985. Biological and biochemical differences between variants of spleen focus-forming virus can be localized to a region containing the 3′ end of the envelope gene. *J. Virol.* 56: 717–722.
9. Li, J. P., A. D. D'Andrea, H. F. Lodish, and D. Baltimore. 1990. Activation of cell-growth by binding of friend spleen focus-forming virus gp55 glycoprotein to the erythropoietin receptor. *Nature*. 343: 762–764.
10. Hoatlin, M. E., S. L. Kozak, F. Lilly, A. Chakraborti, C. A. Kozak, and D. Kabat. 1990. Activation of erythropoietin receptors by friend viral gp55 and by erythropoietin and down-modulation by the murine fv-2r resistance gene. *Proc. Natl. Acad. Sci. USA*. 87:9985–9989.
11. Ruscetti, S. K., N. J. Janesch, A. Chakraborti, S. T. Sawyer, and W. D. Hankins. 1990. Friend spleen focus-forming virus induces factor independence in an erythropoietin-dependent erythroleukemia cell-line. *J. Virol.* 64:1057–1062.
12. Watowich, S. S., H. Wu, M. Socolovsky, U. Klingmuller, S. N. Constantinescu, and H. F. Lodish. 1996. Cytokine receptor signal transduction and the control of hematopoietic cell development. *Annu. Rev. Cell Dev. Biol.* 12:91–128.
13. Ferro, F. E., S. L. Kozak, M. E. Hoatlin, and D. Kabat. 1993. Cell-surface site for mitogenic interaction of erythropoietin receptors with the membrane glycoprotein encoded by friend-erythroleukemia virus. *J. Biol. Chem.* 268:5741–5747.
14. Li, J. P., H. O. Hu, Q. T. Niu, and C. Fang. 1995. Cell-surface activation of the erythropoietin receptor by friend spleen focus-forming virus gp55. *J. Virol.* 69:1714–1719.
15. Yoshimura, A., A. D. D'Andrea, and H. F. Lodish. 1990. Friend spleen focus-forming virus glycoprotein gp55 interacts with the erythropoietin receptor in the endoplasmic-reticulum and affects receptor metabolism. *Proc. Natl. Acad. Sci. USA*. 87:4139–4143.
16. Casadevall, N., C. Lacombe, O. Muller, S. Gisselbrecht, and P. Mayeux. 1991. Multimeric structure of the membrane erythropoietin receptor of murine erythroleukemia-cells (friend-cells)—cross-linking of erythropoietin with the spleen focus-forming virus envelope protein. *J. Biol. Chem.* 266:16015–16020.
17. Showers, M. O., J. C. Demartino, Y. Saito, and A. D. D'Andrea. 1993. Fusion of the erythropoietin receptor and the friend spleen focus-forming virus gp55 glycoprotein transforms a factor-dependent hematopoietic-cell line. *Mol. Cell. Biol.* 13:739–748.
18. Srinivas, R. V., D. R. Kilpatrick, S. Tucker, Z. Rui, and R. W. Compans. 1991. The hydrophobic membrane-spanning sequences of the gp52 glycoprotein are required for the pathogenicity of friend spleen focus-forming virus. *J. Virol.* 65:5272–5280.
19. Watanabe, N., M. Nishi, Y. Ikawa, and H. Amanuma. 1991. Conversion of friend mink cell focus-forming virus to friend spleen focus-forming virus by modification of the 3′ half of the env gene. *J. Virol.* 65:132–137.
20. Constantinescu, S. N., H. Wu, X. D. Liu, W. Beyer, A. Fallon, and H. F. Lodish. 1998. The anemic friend virus gp55 envelope protein induces erythroid differentiation in fetal liver colony-forming units-erythroid. *Blood.* 91:1163–1172.
21. Constantinescu, S. N., T. Keren, W. P. Russ, I. Ubarretxena-Belandia, Y. Malka, K. F. Kubatzky, D. M. Engelman, H. F. Lodish, and Y. I. Henis. 2003. The erythropoietin receptor transmembrane domain mediates complex formation with viral anemic and polycythemic gp55 proteins. *J. Biol. Chem.* 278:43755–43763.
22. Constantinescu, S. N., X. D. Liu, W. Beyer, A. Fallon, S. C. Shekar, Y. I. Henis, S. O. Smith, and H. F. Lodish. 1999. Activation of the erythropoietin receptor by the gp55-p viral envelope protein is determined by a single amino acid in its transmembrane domain. *EMBO J.* 18:3334–3347.
23. Fang, C., E. Choi, L. G. Nie, and J. P. Li. 1998. Role of the transmembrane sequence of spleen focus-forming virus gp55 in erythroleukemogenesis. *Virology*. 252:46–53.
24. Siminovitch, D. J. 1998. Solid-state NMR studies of proteins: the view from static ^{2}H NMR experiments. *Biochem. Cell Biol.* 76:411–422.
25. Ying, W. W., S. E. Irvine, R. A. Beekman, D. J. Siminovitch, and S. O. Smith. 2000. Deuterium NMR reveals helix packing interactions in phospholamban. *J. Am. Chem. Soc.* 122:11125–11128.
26. Sharpe, S., K. R. Barber, and C. W. M. Grant. 2000. Val(659)→Glu mutation within the transmembrane domain of erbb-2: effects measured by H-2 NMR in fluid phospholipid bilayers. *Biochemistry*. 39:6572–6580.
27. Liu, W., E. Crocker, D. J. Siminovitch, and S. O. Smith. 2003. Role of side-chain conformational entropy in transmembrane helix dimerization of glycophorin A. *Biophys. J.* 84:1263–1271.
28. Bloom, M., and I. C. P. Smith. 1985. Manifestations of lipid-protein interactions in deuterium NMR. *In* Progress in Protein-Lipid Interactions. A. Watts and J. H. H. M. De Pont, editors. Elsevier, Amsterdam. 61–88.
29. Smith, S. O., M. Eilers, D. Song, E. Crocker, W. W. Ying, M. Groesbeek, G. Metz, M. Ziliox, and S. Aimoto. 2002. Implications of threonine hydrogen bonding in the glycophorin A transmembrane helix dimer. *Biophys. J.* 82:2476–2486.
30. Rothschild, K. J., and N. A. Clark. 1979. Polarized infrared spectroscopy of oriented purple membrane. *Biophys. J.* 25:473–487.
31. Bradbury, E. M., L. Brown, A. R. Downie, A. Elliott, R. D. B. Fraser, and W. E. Hanby. 1962. The structure of the ω-form of poly-β-benzyl-l-aspartate. *J. Mol. Biol.* 5:230–247.
32. Marsh, D., M. Muller, and F. J. Schmitt. 2000. Orientation of the infrared transition moments for an α-helix. *Biophys. J.* 78:2499–2510.
33. Marsh, D., and T. Pali. 2001. Infrared dichroism from the x-ray structure of bacteriorhodopsin. *Biophys. J.* 80:305–312.
34. Smith, S. O., R. Jonas, M. Braiman, and B. J. Bormann. 1994. Structure and orientation of the transmembrane domain of glycophorin A in lipid bilayers. *Biochemistry*. 33:6334–6341.
35. Bak, M., J. T. Rasmussen, and N. C. Nielsen. 2000. Simpson: a general simulation program for solid-state NMR spectroscopy. *J. Magn. Reson.* 147:296–330.
36. Adams, P. D., D. M. Engelman, and A. T. Brunger. 1996. Improved prediction for the structure of the dimeric transmembrane domain of glycophorin A obtained through global searching. *Proteins*. 26:257–261.
37. Popot, J. L., and D. M. Engelman. 2000. Helical membrane protein folding, stability, and evolution. *Annu. Rev. Biochem.* 69:881–922.
38. Eilers, M., A. B. Patel, W. Liu, and S. O. Smith. 2002. Comparison of helix interactions in membrane and soluble α-bundle proteins. *Biophys. J.* 82:2720–2736.
39. Batchelder, L. S., C. E. Sullivan, L. W. Jelinski, and D. A. Torchia. 1982. Characterization of leucine side-chain reorientation in collagen-fibrils by solid-state 2H NMR. *Proc. Natl. Acad. Sci. USA*. 79:386–389.
40. Bowie, J. U. 1997. Helix packing in membrane proteins. *J. Mol. Biol.* 272:780–789.
41. Chothia, C., M. Levitt, and D. Richardson. 1981. Helix to helix packing in proteins. *J. Mol. Biol.* 145:215–250.
42. Eilers, M., S. C. Shekar, T. Shieh, S. O. Smith, and P. J. Fleming. 2000. Internal packing of helical membrane proteins. *Proc. Natl. Acad. Sci. USA*. 97:5796–5801.
43. Javadpour, M. M., M. Eilers, M. Groesbeek, and S. O. Smith. 1999. Helix packing in polytopic membrane proteins: role of glycine in transmembrane helix association. *Biophys. J.* 77:1609–1618.
44. MacKenzie, K. R., J. H. Prestegard, and D. M. Engelman. 1997. A transmembrane helix dimer: structure and implications. *Science*. 276: 131–133.

45. Lemmon, M. A., J. M. Flanagan, H. R. Treutlein, J. Zhang, and D. M. Engelman. 1992. Sequence specificity in the dimerization of transmembrane α-helices. *Biochemistry*. 31:12719–12725.

46. Constantinescu, S. N., L. J. S. Huang, H. S. Nam, and H. F. Lodish. 2001. The erythropoietin receptor cytosolic juxtamembrane domain contains an essential, precisely oriented, hydrophobic motif. *Mol. Cell.* 7:377–385.

47. Russ, W. P., and D. M. Engelman. 1999. TOXCAT: a measure of transmembrane helix association in a biological membrane. *Proc. Natl. Acad. Sci. USA*. 96:863–868.

48. Gurezka, R., R. Laage, B. Brosig, and D. Langosch. 1999. A heptad motif of leucine residues found in membrane proteins can drive self-assembly of artificial transmembrane segments. *J. Biol. Chem.* 274: 9265–9270.

49. Leeds, J. A., D. Boyd, D. R. Huber, G. K. Sonoda, H. T. Luu, D. M. Engelman, and J. Beckwith. 2001. Genetic selection for and molecular dynamic modeling of a protein transmembrane domain multimerization motif from a random Escherichia coli genomic library. *J. Mol. Biol.* 313:181–195.

50. Taylor, G. M., and D. A. Sanders. 1999. The role of the membrane-spanning domain sequence in glycoprotein-mediated membrane fusion. *Mol. Biol. Cell.* 10:2803–2815.

51. Hofmann, M. W., K. Weise, J. Ollesch, P. Agrawal, H. Stalz, W. Stelzer, F. Hulsbergen, H. de Groot, K. Gerwert, J. Reed, and D. Langosch. 2004. *De novo* design of conformationally flexible transmembrane peptides driving membrane fusion. *Proc. Natl. Acad. Sci. USA*. 101:14776–14781.